Development of an *in situ* procedure to evaluate the reticulo-rumen morphology of sheep selected for divergent methane emissions

S. J. Waite 1, J. Zhang 1, J. E. Cater 2, G. C. Waghorn a, W. E. Bain 3, J. C. McEwan 3 and V. Suresh 1,2

[1] *Auckland Bioengineering Institute, University of Auckland, Auckland, New Zealand.*

[2] *Department of Engineering Science, University of Auckland, Auckland, New Zealand.*

[3] *AgResearch Invermay, Mosgiel, New Zealand.*

[a,] *Present address: 6 Berkley Avenue, Hamilton, New Zealand.*

Corresponding author: Dr Vinod Suresh. Email: v.suresh@auckland.ac.nz

Short title: Reticulo-rumen shape in high and low CH4 sheep.

Abstract

Published studies have shown that methane yield (g CH_4/kg dry matter (**DM**)) from sheep is positively correlated with the size (volume and surface area) of the reticulo-rumen (**RR**) and the weight of its contents. However, the relationship between methane yield and RR shape has not been investigated. In this work, shape analysis has been performed on a dataset of computerised tomography (**CT**) scans of the RR from sheep having high and low methane yields (n=20 and n=17 respectively). The three-dimensional geometries of the RRs were reconstructed from segmented scan data and split into three anatomical regions. An iterative fitting technique combining radial basis functions and principal component (**PC**) fitting was used to create a set of

consistent landmarks which were then used as variables in a PC analysis to identify shape variation within the data. Significant size differences were detected for regions corresponding to the dorsal and ventral compartments between sheep with high and low CH_4 yields. When the analysis was repeated after scaling the geometries to remove the effect of size, there was no significant shape variation correlating with CH_4 yield. The results have demonstrated the feasibility of CT based computational shape determination for studying the morphological characteristics of the RR and indicate that size, but not shape, correlates with methane yield in sheep.

Keywords: Reticulo-rumen, Shape Analysis, Methane Yield, Statistical Shape Modelling, Principal Component Analysis.

Implications

Research has shown that there is a link between reticulo-rumen size of sheep and the amount of methane produced from the same amount of feed eaten. However, it is not known if the shape of the rumen differs between individuals. This study describes the application of computational techniques for the analysis and comparison of complex geometries in conjunction with images from computed tomography (CT) to determine morphological (shape) characteristics of the rumen. In contrast to previous studies of rumen morphology, this approach provides information on both size-dependent and size-independent characteristics.

Introduction

The reticulo-rumen (**RR**) is the first compartment in the digestive system of ruminants. Although it performs a similar function in a range of species, breeds and

individuals, its morphological features – e.g. the total size/capacity of the organ, the relative volume of its compartments, papillation patterns and motility vary widely, for example between concentrate selectors and roughage eaters (Hofmann, 1989; Clauss *et al*., 2009). These differences are thought to be evolutionary adaptations to differences in the physical characteristics and chemical composition of feed, affecting functions such as retention times, stratification of RR contents (separation into solid, fluid and gas fractions) and fluid passage rates (Clauss *et al*., 2010a and 2010b). Variations in morphology have also been linked to variation in function, for example, in relation to susceptibility to legume bloat (Waghorn and Reid, 1984).

The RR is a complex multi-compartmental organ that consists of six sacs separated by tissue folds and muscular pillars (**Figure 1**) that help to hold the shape and enable contractions (Wyburn, 1979). The dorsal and ventral sacs are the largest compartments and contribute most of the RR volume. Contractions of the caudo-dorsal and caudo-ventral blind sacs drive digesta towards the cranial sac and the reticulum, while contractions of the reticulum (which can be considered as a separate organ) and the cranial sac drive digesta flow caudally (Waghorn *et al*., 1977). Digesta is a heterogeneous mixture of plant fragments, saliva and an anaerobic microflora, and its behaviour is dominated by mixing, floatation, sedimentation (Sutherland, 1988). Contents can exit the RR through the reticulo-omasal orifice to the omasum (Sellers and Stevens, 1966; Wyburn, 1979).

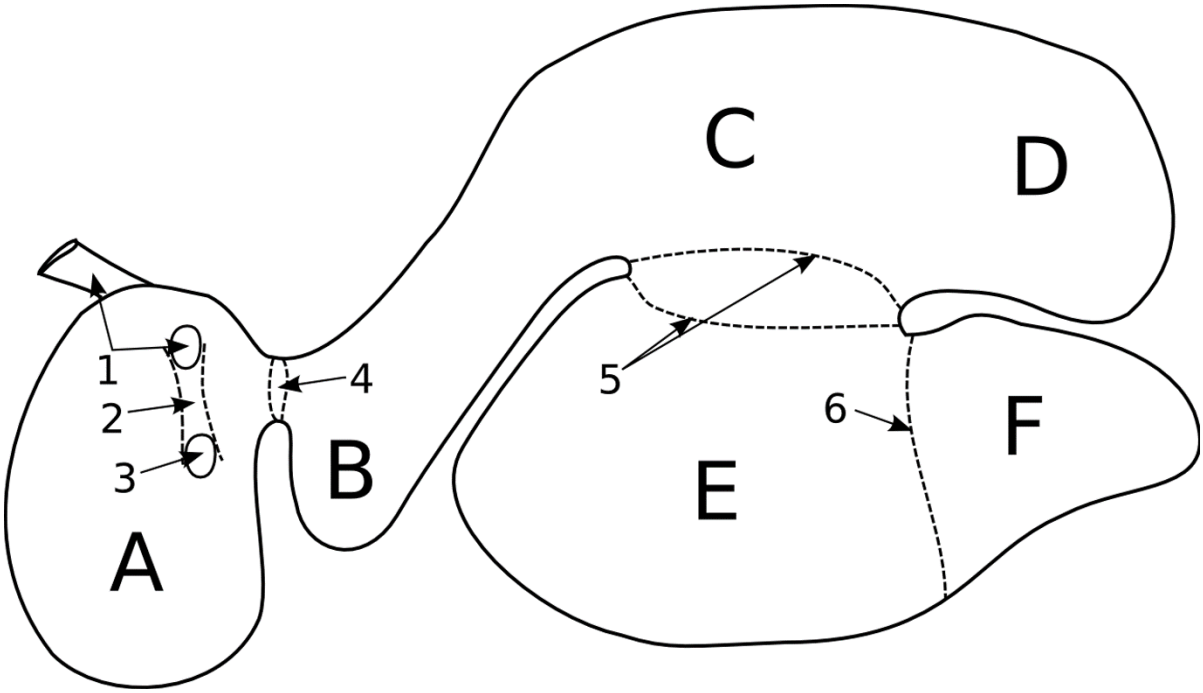

Figure 1 Illustration of the reticulo-rumen internal geometry for sheep. A) reticulum, B) cranial sac/atrium, C) dorsal sac, D) caudo-dorsal blind sac, E) ventral sac, F) caudo-ventral blind sac. 1) oesophagus, 2) reticular groove, 3) reticulo-omasal orifice, 4) reticulo-rumen orifice, 5) left and right longitudinal pillars, 6) caudo-ventral pillar.

Shape analysis is a technique that is often used to quantify morphological and evolutionary variation of species (Wiley *et al*., 2005; Webster and Sheets, 2010). It has been used to investigate the effect of variables such as gender, age and disease on shape variations, such as for bones in humans (Zhang *et al*.,2013; Schneider *et al*., 2015) and can be used with non-morphometric variables in parsimony based cladistics studies to test evolutionary relationships between taxa in population models (Bogdanowicz *et al*., 2005; Rosenberger, 2011). Shape analysis of RR compartments could identify differences between individuals that may affect digesta flow patterns and mixing, and thus influence passage of fluid (with small particulate and suspended/dissolved dry matter (**DM**)) from the RR, affecting digesta kinetics and methanogenesis.

The procedures developed here were motivated by measurements showing a link between RR physiology and variation in methane (**CH_4**) yield (g CH_4/kg DM) between sheep fed the same diet. Such variation was largely explained by the organic matter fill and fractional outflow rate of particulate matter from the RR (Pinares *et al*., 2003). More recently, Hammond *et al*. (2014) and Pacheco *et al*.(2014) have associated increased intakes with reduced CH_4 yields and a faster passage through the RR (reduced residence time), sometimes in association with reduced digestibility (Pinares-Patino *et al*., 2011). Selection of sheep having divergent CH_4 yield have established a heritability of 0.13 ± 0.03 (Pinares-Patino *et al*., 2013) and preliminary measurements have shown differences in the surface area, volume, and composition of digestive contents in the RR of sheep with divergent CH_4 yields (Goopy *et al*., 2013; Bain *et al*., 2014). However, there has been no corresponding study of shape variations between high and low CH_4 yield animals. Shape variations may affect CH_4

yield by influencing outflow rate and mixing. For example the depth of the reticulum relative to its width and height may influence the size of digesta particles that are transferred through the ROO, due to the density sorting mechanics described by Clauss et al., (2010a), effecting residence time. It has also been suggested that low concentrations of hydrogen in the RR can lead to increased CH_4 yield due to thermodynamic effects on fermentation reactions (Janssen 2010). Differences in the shape of RR compartments may alter the degree of mixing during RR contraction and lead to variations in hydrogen concentrations in the digesta. In this work, we developed methods to quantitatively assess RR shape and analysed RR imaging data from high and low CH_4 yield sheep to determine if shape differences contribute to variation in CH_4 yield.

Shape is defined as the geometric information that remains when location, scale and rotational effects are removed (Kendall, 1977). Traditionally, shape analysis uses points or other elements (landmarks) that correspond to the same biological feature on different individuals or samples to characterise shape (Bookstein, 1985). The complex curvature of the RR surface and its deformable nature make it difficult to identify biological landmarks consistently across individuals. Therefore, an alternative approach was employed from statistical shape modelling (Heimann and Meinzer, 2009), where a source shape is computationally deformed to match each RR in order to identify corresponding points on each individual. This approach minimises subjective selection by the user and maximizes repeatability allowing for the evaluation of shape variation between selection lines. The application of this method to the RR is novel and provides a consistent and quantitative approach for morphological analysis. The methods are developed and used to investigate if shape

differences in sheep RR geometry are significant for animals known to differ in CH_4 yield.

Material and methods

The data set used in this research was obtained from 45 female sheep, aged approximately 2 years 10 months, located at AgResearch Invermay (Mosgiel, New Zealand. The study was carried out in strict accordance of the guidelines of the 1999 New Zealand Animal Welfare Act and was approved by the AgResearch's Invermay Animal Ethics committee (applications AE12206 and AE12963). The animals had been identified for divergence in CH_4 yield (Bain *et al*., 2014) and Pinares-Patino *et al*., (2013) has described the overall selection process and estimation of heritability, based upon 1250 ewes aged 8-10 months fed measured amounts of pelleted lucerne (*Medicago sativa* L) and screened in respiration chambers over several years. Forty five animals that had the highest CH_4 yields (18.68 ± 1.04 g/kg DMI) and lowest yields (17.23± 1.21 g/kg DMI) when fed similar intakes of pellets, were retained and used for measurements of RR morphology. Furthermore, Pinares-Patino *et al*, 2011b had shown that divergence in CH_4 yield from sheep fed pellets was retained when they were fed fresh pasture. A preliminary analysis of the RR volume and digesta weights was presented by Bain *et al*., (2014).

Computed tomography (CT) measurements (Siemens Somatom ARC, Siemens Medical System, Erlangen, Germany) were undertaken on the selected animals after grazing pasture *ad libitum*. Measurements were made on the 45 animals (21 with low CH_4 yields and 24 with high CH_4 yields) over 4 days and their BW (71.61±5.88 and 75.25±7.74 (mean±SD) kg for the respective groups) recorded when removed from

grazing at 0900h. The CT procedure involved sedation with Xylase20 (20 mg/mL), as an intra-muscular injection at 0.01-0.02 mg active ingredient (xylazine)/kg BW, and placement in a modified polyvinyl chloride cradle (400 mm diameter pipe) for scanning (Bain *et al*., 2014). Animals were placed in a prone position with the hind legs extended caudally and forelegs folded under the chest. The RR scans were performed starting at the 6^{th} and 7^{th} thoracic vertebrae, through to the 6^{th} lumbar vertebrae. Images were taken at 15mm intervals with a 450mm field of view. The process took approximately 20 minutes per animal and the time elapsed between removal from pasture and scanning (time removed from pasture (**TRP);** 4.29±1.51 and 4.95±1.78 hours for low and high yielding respectively) was recorded.

Surface Reconstruction

Animal data existed for measurements over two years, 2012 and 2013. The 2013 scanning data was selected as the animal position was more consistent between scans. This group contained 39 of the original 45 animals. CT images consisted of a series of 2D transverse planes which were manually segmented using the software package Stradwin v5.3 (http://mi.eng.cam.ac.uk/-rwp/stradwin) and interpolated using marching tetrahedra (Treece et al., 1999). Slices that contained significant contractive motion of the RR were removed before surface interpolation. Animals that exhibited body motion during scanning were removed from the study (n=2), resulting in 20 reconstructed high CH_4 yielding animals, and 17 low yield. The RR surface consists of a series of tissue folds that separate the organ into various regions and compartments. These folds make it difficult to enforce point correspondence of the RR between different animals. Therefore, the RR was broken into three sections shown in **Figure 2**, comprising of the reticulum and cranial sac (anterior), dorsal sac

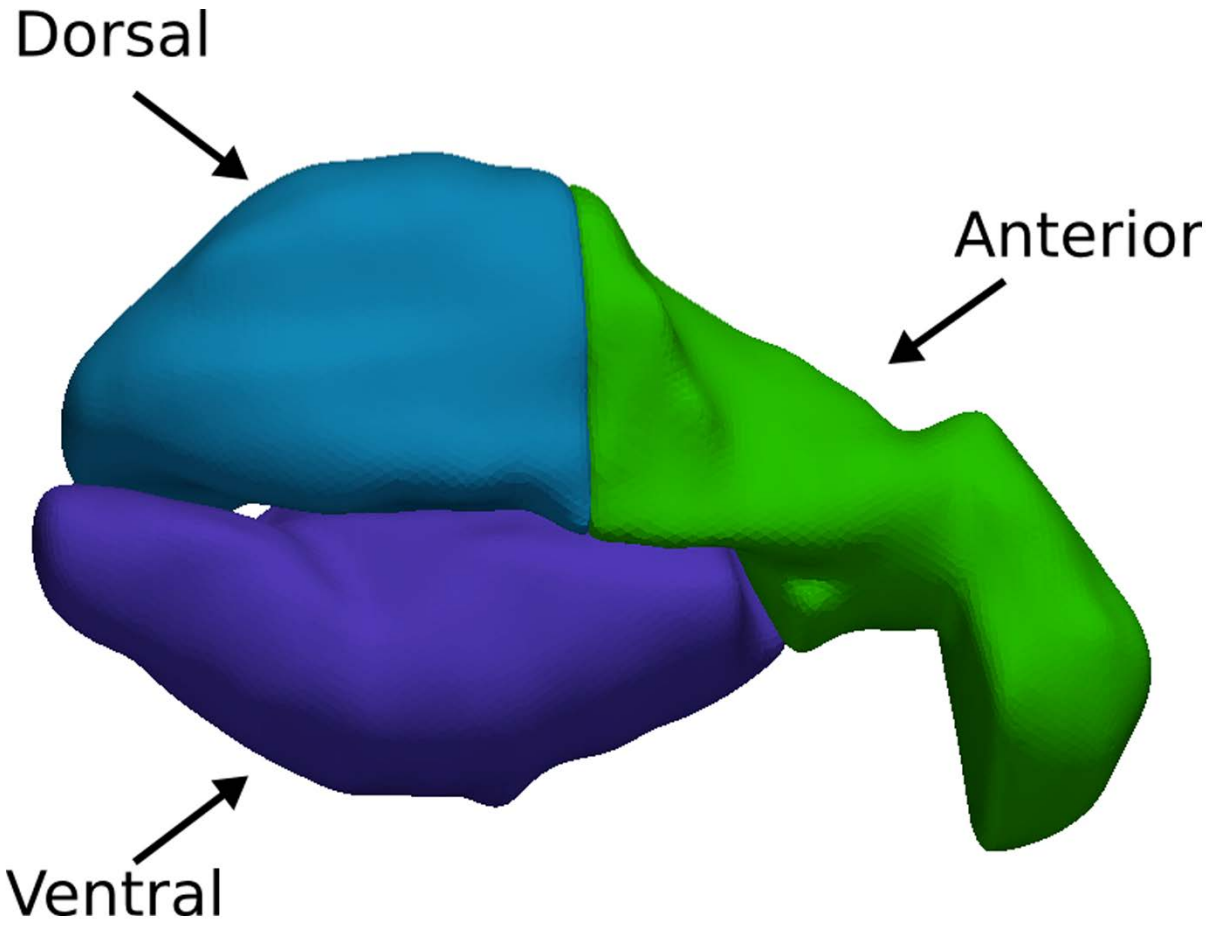

Figure 2 Sectioning of the reticulo-rumen in sheep. Blue: the dorsal and caudal dorsal blind sac (dorsal). Green: the reticulum and cranial sac (anterior). Purple: the ventral and caudal ventral blind sac (ventral).

and caudal dorsal blind sac (dorsal), and the ventral and caudal ventral blind sac (ventral). This method also helps to remove the effects of local twisting that occurs along the length the RR due to the positioning of the animal during scanning.

Landmarking.

To create a series of meshes (connected points that form a geometric surface) with corresponding points or landmarks for shape analysis, an iterative scheme was used combining radial basis functions (**RBF**) and principal component (**PC**) fitting. The RBF method involves the deformation of a source mesh to a target mesh via nearest neighbour searching, in which the closet target point for a given source point is found, and the mesh deformed to minimise this distance [Deng et al 2010]. PC fitting involves the deformation of a mean shape along a select number of principal components or shape axes to again minimise the nearest neighbour distance. PC fitting offers a more constrained fit than RBFs, but with less accuracy in matching topology.

In the first step, a mesh was selected at random from the sample data set as the source and the points (roughly 20,000 from the surface reconstruction step) were fitted to all other meshes using RBF. The mean shape from this initial fit was then calculated and the process was repeated once with the mean shape as the source to improve the quality of fit.

The second step involved an iterative combination of PC and RBF fitting. Principal component analysis (**PCA**) was carried out on the output from the previous step and the first 5 PCs were used to deform the mean shape to each of the sample meshes

to provide an initial approximation. This was followed by a RBF fit to improve topological accuracy. A new mean shape and PCs were then calculated and the procedure repeated until a sufficient level of convergence was obtained. An example of the resulting point correspondence for the anterior region is shown in **Figure 3**. Procedures were performed using the open source python library GIAS2 (Geometry Image-Analysis Statistics) (Zhang et al., 2016). The quality of fit was determined from maximum and root mean squared (**RMS**) Hausdorff distance between the fitted and target surface.

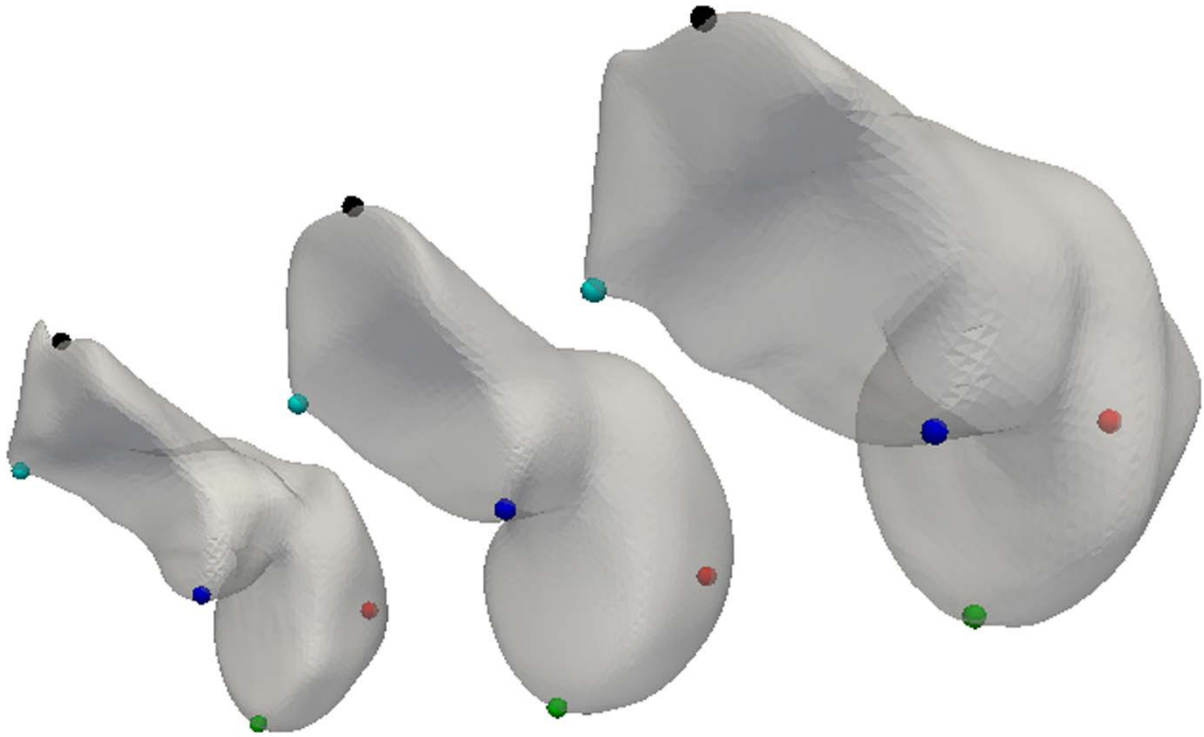

Figure 3 Example of point correspondence after iterative radial basis function and principal component fitting for the anterior section in the reticulum rumen in sheep. The middle subject is the mean shape that has been deformed to fit the two example subjects on its left and right. Physiological points have been manually identified as nodes on the mean shape and highlighted as spheres, corresponding by colour between meshes.

Statistical Analysis

Principal component analysis (PCA) is a technique that can be used to reduce the dimensionality of data sets that depend on a large number of possibly correlated variables by identifying a smaller set of uncorrelated variables (principal components or PCs) that capture the essential features of the data (Zelditch 2004). Here PCA was used to describe the RR geometry information contained in the large number of landmarks with a smaller number of PCs or shape modes. General Procrustes alignment (**GPA**) was used to remove rotations, translations and scaling (normalising the vertex coordinates by centroid size) from the geometries. GPA and PCA operations were performed using the GIAS2 package. The sample geometries have a score associated with each PC, which can be used to reconstruct the shape as a weighted, linear combination of the components added to the mean.

PCA produces as many PCs as the number of samples in the data set, not all of which hold meaningful shape information. Dimension reduction was performed using a broken stick method (Jackson, 1993; Cangelosi, 2007) to select the important PCs to be retained for statistical analysis in R. Univariate Welch two-sample t-tests were used to test significance between the retained PCs and for high and low CH_4 yield. Logistic regression was then performed to investigate the effect of incorporating covariates (BW, TRP and day of scanning). Only shape modes that are significant under both univariate and logistic regression ($P<0.05$) were deemed significant to the hypothesis. The physical meaning of significant shape modes are interpreted by deforming the mean RR shape along the PC axis by two standard deviations for visualisation.

Results

Anterior region

The mean shape of the anterior region of the RR was found to converge after 3 fitting iterations, with an average maximum and RMS fitting error of 2.4 ± 1.9mm and 0.22 ± 0.17mm respectively. When size was included in the PCA, the first component contributed 44.7% of the total variation (**Figure 4**). When this component was inspected it was found to correspond to a size scaling of the anterior region. A univariate t-test indicated no significant difference in PC score value between high and low methane yielding animals. When logistic regression was performed to include covariates, the anterior region size was still found to be insignificant. When size was removed from the data set, the first 5 PCs were deemed important for statistical analysis and were responsible for 63% of the shape variation shown in **Figure 5**. These shape modes consisted of changes in the relative sizes of the cranial sac and reticulum, as well as changes in anterior length and narrowing of the connection to the dorsal sac. A visual representation of the first 3 shape components can be seen in **Figure 6**.No significant difference was detected between any of the shape PCs between high and low methane yielding animals.

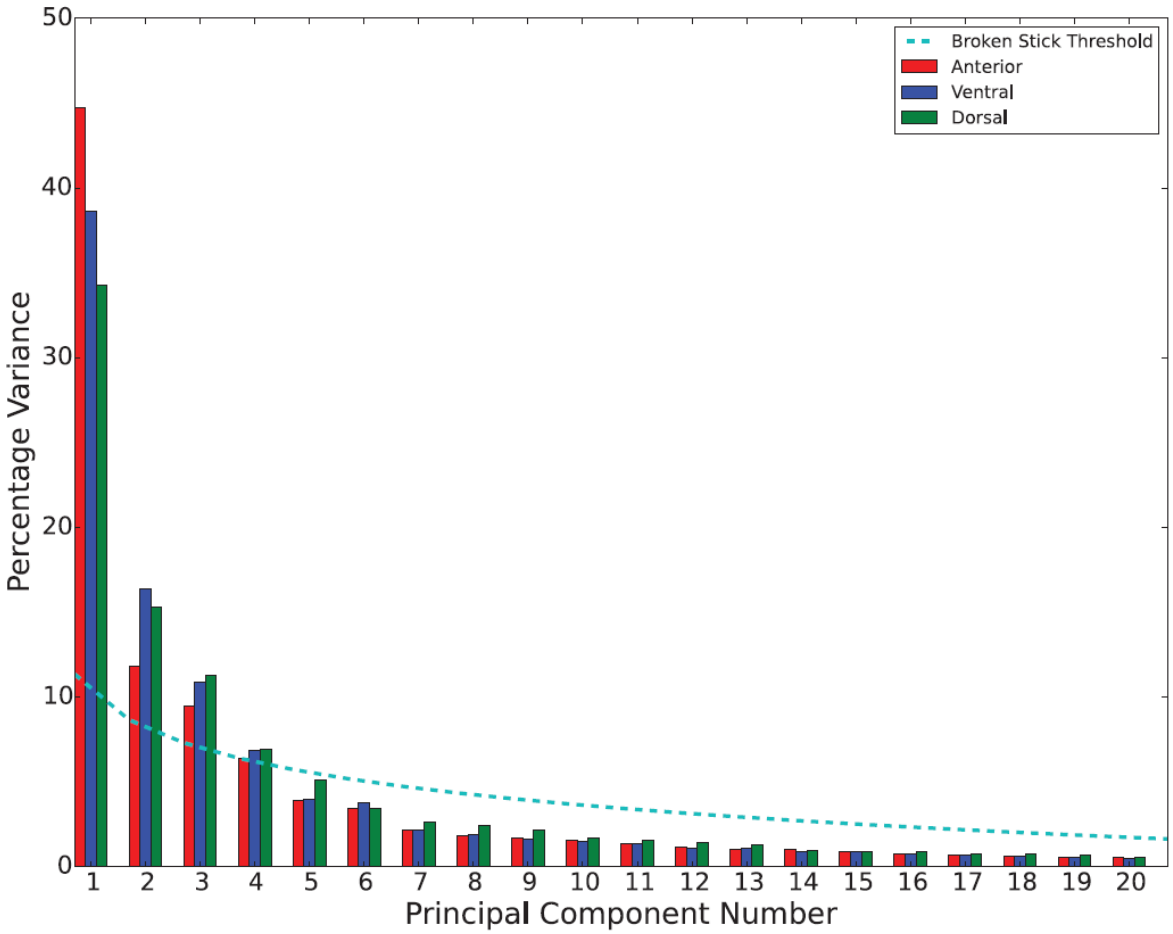

293

294 **Figure 4** Percentage variance when size is included in the principal component

295 analysis of each segmented region; the anterior (red), ventral (blue), and dorsal

296 (green) reticulo-rumen compartments in sheep.

297

298

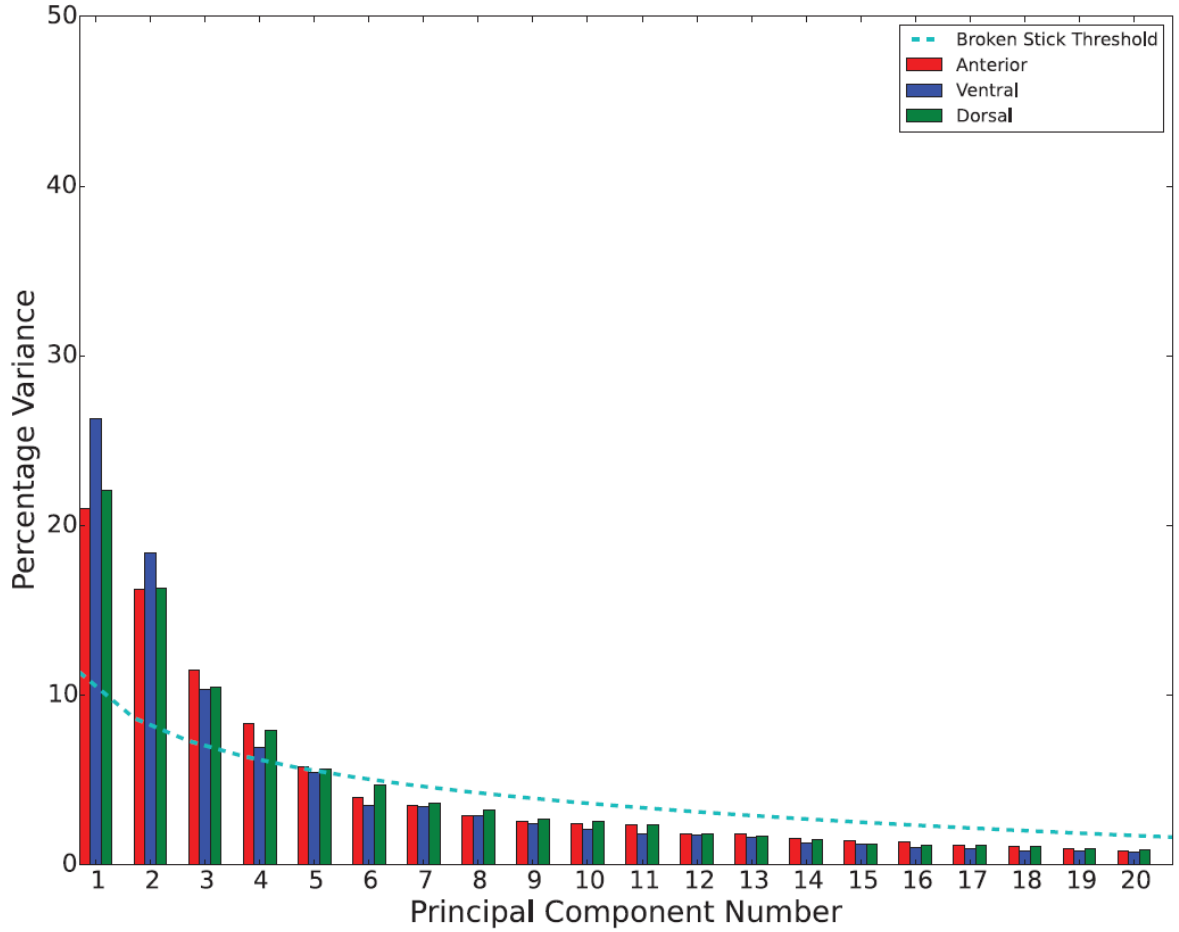

299

300 **Figure 5** Percentage variance when size is removed from the principal component

301 analysis of each segmented region; the anterior (red), ventral (blue), and dorsal

302 (green) reticulo-rumen compartments in sheep.

303

304

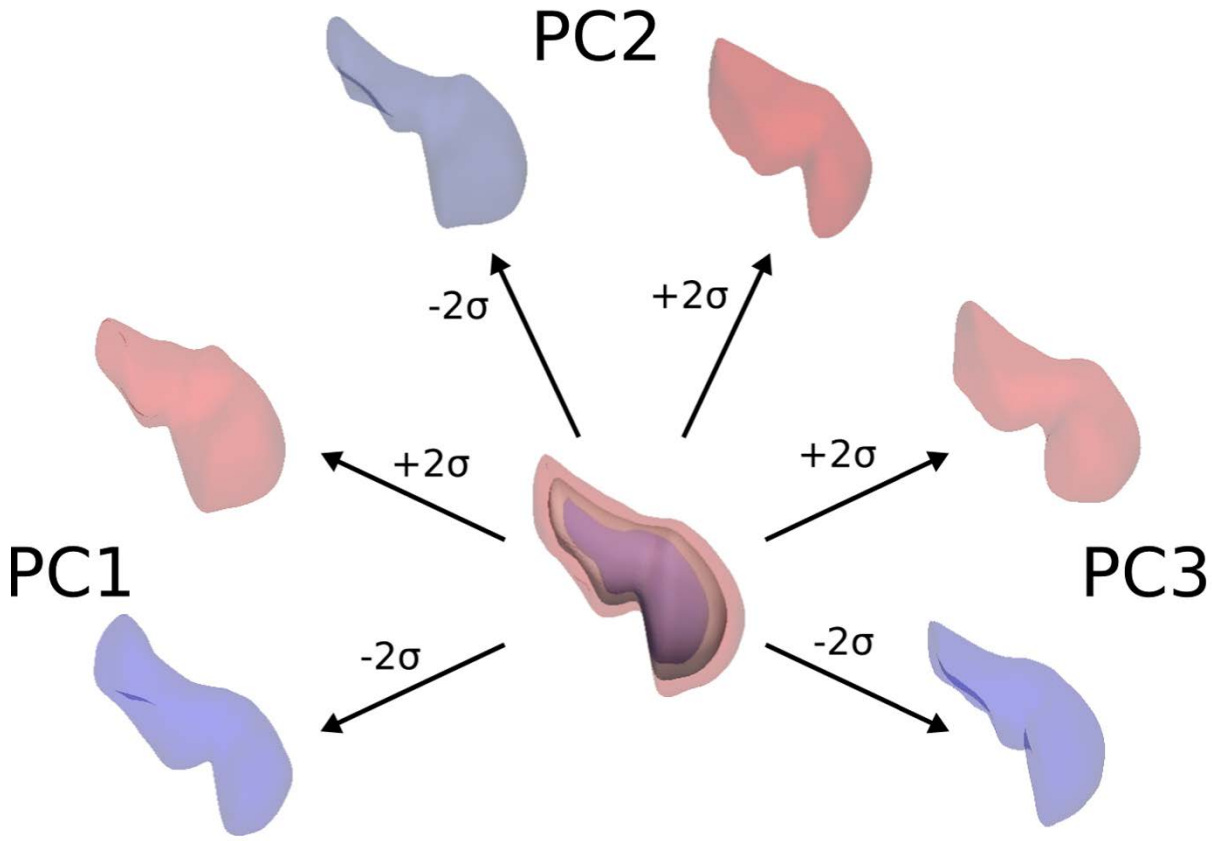

Figure 6 The size component (centre) of the anterior reticulo-rumen region in sheep overlaid on the mean shape (sold grey), and the first three shape components PC1 (left), PC2 (top) and PC3 (right), which have been deformed by ± two standard deviations (σ).

Dorsal region

The mean shape of the dorsal region converged after 4 fitting iterations, with an average maximum and RMS fitting error of 1.8 ± 1.6mm and 0.27 ± 0.25mm respectively. The first PC, corresponding to the size of the dorsal region, contributed 38.6% of the total sample variation shown in **Figure 4**. A univariate t-test indicated a significant difference (P=0.009) for this component between the low and high emitting groups. When logistic regression was performed to include covariates, the dorsal size was still deemed significant (P=0.012, R^2=0.19). Interpreting the physical meaning of the size component, high emitters are found to have a negative mean score, which corresponds to increased size from the mean shape. Conversely, the low yielding group have a positive mean score corresponding to decreased size from the mean shape. An example of the size component can be seen in **Figure 7**. When size was removed from the dorsal samples the first four shape components were deemed important for statistical analysis and were responsible for 57% of the shape variation, as shown in **Figure 5**. Shape modes included elongation of the whole dorsal region, as well as relative size differences between the dorsal sac and the caudal dorsal blind sac. A visual representation of the first 3 shape components can be seen in **Figure 7**. No significant difference was detected for any of the mean PC scores for high and low methane yield.

Ventral region

The mean shape of the ventral region converged after 4 fitting iterations, with an average maximum and RMS fitting error of 2.4±1.5mm and 0.36 ± 0.32mm respectively. The size component of the ventral region contributed 34.3% of the total sample variation shown in **Figure 4**. A univariate t-test indicated a significant

difference (P=0.0002) between the mean PC score for low and high emitting groups. When logistic regression was performed to include covariates, the ventral size was still deemed significant (P=0.002 R^2=0.32). Interpreting the physical meaning of the component scores, high emitters were found to have a negative mean score corresponding to an increase in size from the mean shape, while low emitters have a positive mean score, a decrease in size from the mean shape, as shown in **Figure 8**. When size was removed from the samples and thresh-holding applied, the first four shape components were deemed important for statistical analysis and were responsible for 73% of the shape variation as shown in **Figure 5**. Shape modes included elongations of the caudal ventral blind sac, an increase in ventral sac depth/height, as well as the relative angle between the two compartments. A visual representation of the first 3 shape components can be seen in **Figure 8**. No significant difference was detected for any of shape scores for high and low methane yield.

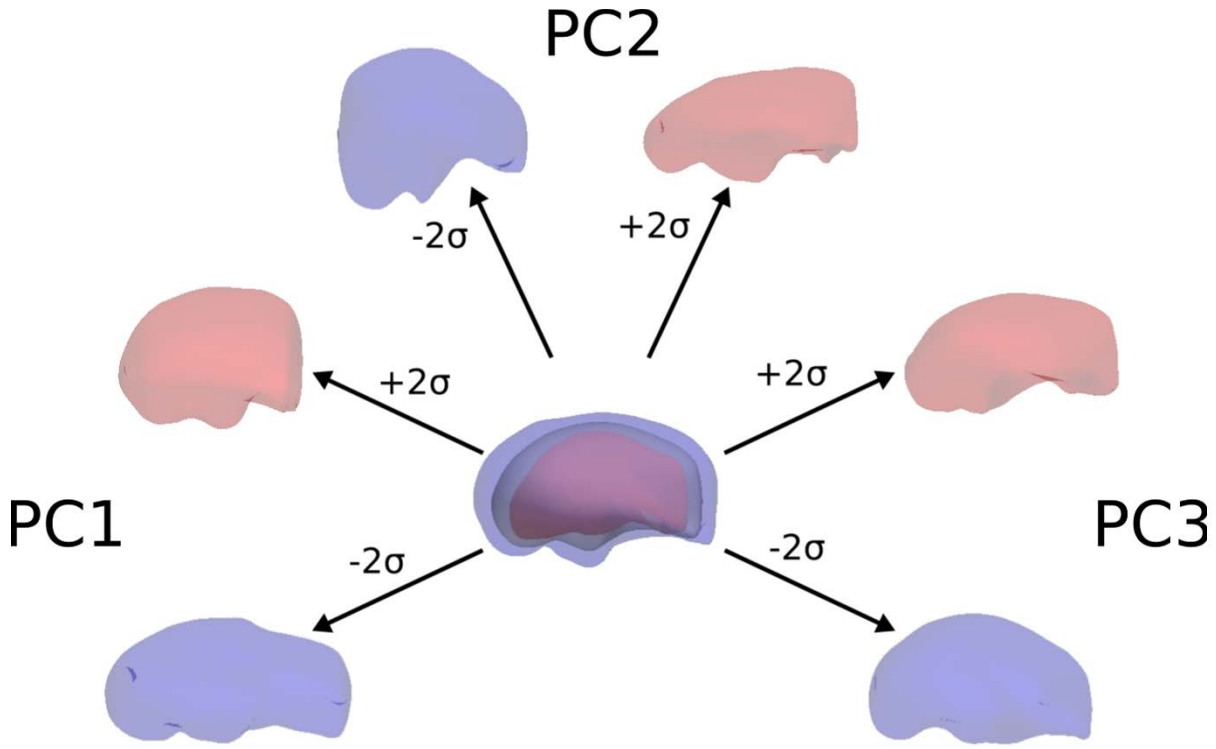

Figure 7 The size component (centre) of the dorsal reticulo-rumen region in sheep overlaid on the mean shape (sold grey), and the first three shape components PC1 (left), PC2 (top) and PC3 (right), which have been deformed by ± two standard deviations (σ).

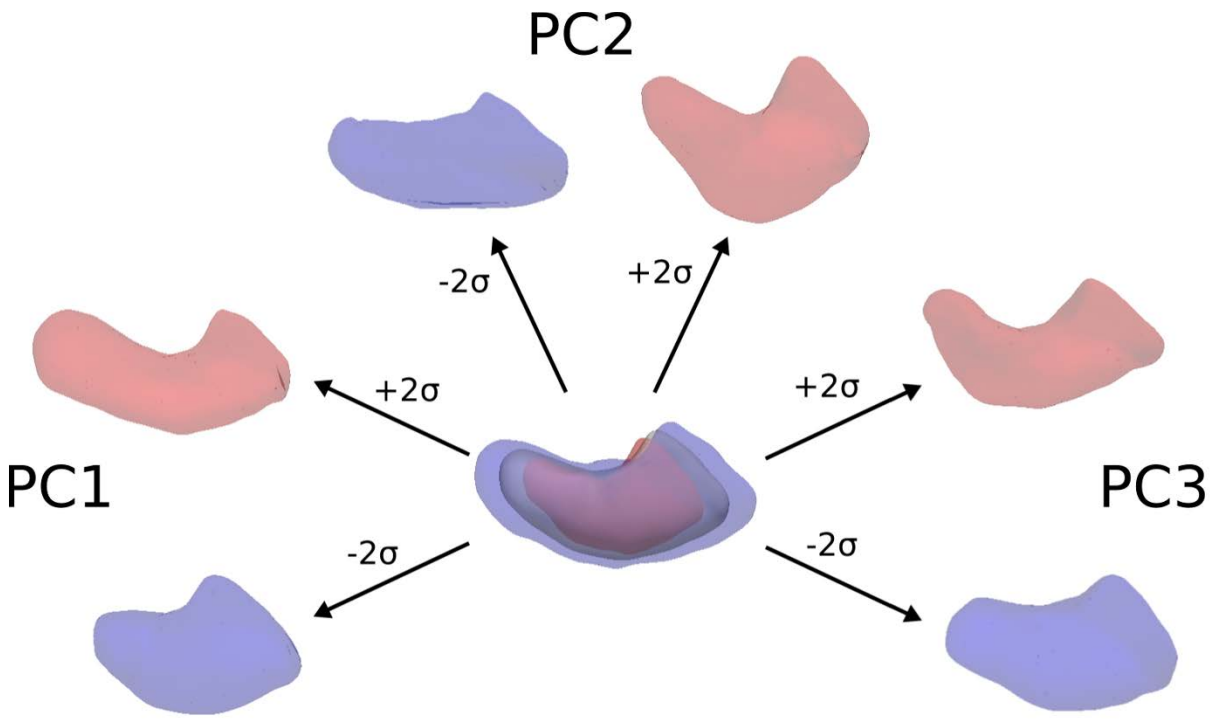

Figure 8 The size component (centre) of the ventral reticulo-rumen region in sheep overlaid on the mean shape (sold grey), and the first three shape components PC1 (left), PC2 (top) and PC3 (right), which have been deformed by ± two standard deviations (σ).

Discussion

The PCA was first performed on the sample groups with size/volume included in the geometric information to determine if the method could detect size as a significant mode of variation and if a difference could be detected between high and low CH_4 yield groups, as found by Bain *et al* (2014) and Goopy (2014). Results showed that the mode with the largest contribution (PC1) for all three regions was indeed related to overall size. A univariate comparison indicated that the high CH_4 group has a larger dorsal and ventral region than the low CH_4 group (P=0.009 and 0.0002 respectively), despite similar BW which may be related to the link between digesta residence times and CH_4 emissions for a range of feeds previously reported (Pinares-Patiño *et al.,* 2003; Hammond *et al.,* 2014; Pacheco *et al.,* 2014).

While the size of the anterior region, corresponding to the reticulum and cranial sacs accounted for 45% of the total sample variation, no significant difference was detected between group means for high and low yielding animals.

When the analysis was repeated after scaling the RR geometries to remove size, the first 4-5 shape components were found to contribute more than 50% of the total sample variation. While these modes represented physiologically meaningful shape differences, no significant difference could be detected between high and low CH_4 yielding animals for any of the three regions of interest. From these results, we conclude that RR size is correlated with methane yield, but we find no significant correlation between the shape of the RR, and methane yield. While shape differences account for a significant percentage of variation within the tested animals, we could not detect any systematic differences between the high and low methane

yielding groups. It may be the case that true shape differences are difficult to detect due to the nature of the RR and confounding factors discussed below.

Challenges in this procedure

Determining the true shape of the RR is complicated by the highly deformable nature of the organ and its domination of the viscera in the abdominal cavity. As a consequence, it has considerable interactions with other internal structures, such as the spleen, omasum, abomasum, intestines, and abdominal wall. This means that the orientation and positioning of the animal in the CT scanner can cause significant distortions to the RR shape as well as local twisting of the organ, between the reticulum, rumen and blind sacs. In addition, internal gas pressure and digestive fill could have a significant influence on RR shape. These factors add noise to the PCA and may mask true differences in shape between high and low CH_4 yield animals. While the methods used in this study attempted to address the issue of relative twisting between compartments of the RR, future work could include more pre-processing of the imaging data to remove identifiable RR distortions.

Other possible sources of error include scan quality and alignment of the geometries prior to PCA. The CT scans were performed with a 15mm slice plane interval; this can cause a loss of information when significant curvature occurs between slice planes, such as at the end of a compartment at the reticulum or caudal blind sacs. The distance between these slice planes, as well as the contrast quality used to define the interface between the tissue surface and the RR interior, can create reconstruction artefacts that are difficult to remove.

Alignment operations performed on the reconstructed geometries (translation and rotation performed using GPA) also contribute to the overall noise. Each shape is scaled by centroid size and translated to share the same reference centroid position. Rigid body rotations are then performed to minimise the Procrustes distance between the different geometries. However, the shapes cannot be perfectly matched to each other and so the alignment of shapes is sensitive to the initial orientation, giving rise to an apparent shape difference.

Summary

We have adopted the techniques of statistical shape modelling to investigate RR morphology in sheep. The approach offers a method for comparing geometries that are complex in shape, and lack common physiological features for applying traditional landmarks via an automatic fitting process. This allows us to perform quantitative analysis of shape differences for the RR of sheep. Using these techniques, we have detected significant differences in size for the dorsal and ventral regions of the RR between high and low CH_4 yielding sheep. When size was removed by scaling the geometries, our analysis detected no significant shape difference between high and low CH_4 yield animals. This suggests that observed differences in outflow rates and residence times are independent of shape variations within the RR.

Acknowledgements

This study was funded by the Agricultural Marketing and Research Development Trust (AGMARDT) and DairyNZ through scholarship support to Stephen James Waite. The experimental work was funded by the Agricultural Marketing and

Research Development Trust AGMARDT and DairyNZ through scholarship support to Stephen J Waite. Experimental studies were funded by the Pastoral Greenhouse Gas Research Consortium, Sustainable Land Management and Climate Change and the New Zealand Agricultural Greenhouse Gas Research Centre. The animals themselves were part of the Ovita partnership and the related Central Progeny Test: both funded in part or whole by Beef + Lamb New Zealand. Thanks also to the Central Progeny Test collaborating organisations: AgResearch Woodlands especially Kevin Knowler, On Farm Research especially Paul Muir, Lincoln University especially Chris Logan and AbacusBio Ltd especially Neville Jopson.

Declaration of interest

This study was performed with no conflict of interest.

Ethics statement

The study was carried out in strict accordance of the guidelines of the 1999 New Zealand Animal Welfare Act and was approved by the AgResearch's Invermay Animal Ethics committee (applications AE12206 and AE12963).

Software and data repository resources

None of the data were deposited in an official repository.

References

Bain W, Pinares-Pantino CS, McEwan JC 2014. Rumen differences between sheep identified as being low or high methane emitters. In Proceedings of the 10th World

480 Congress of Genetics Applied to Livestock Production, 17-22 August 2014,
481 Vancourver BC, Canada, pp. 1-3.
482
483 Bogdanowicz W, Juste J, Owen RD, Sztencel A 2005. Geometric morphometrics and
484 cladistics: testing evolutionary relationships in mega- and microbast. Acta Chiroptero-
485 logica 7, 39–49.
486
487 Bookstein FL, Chernoff B, Elder R, Humphires J, Smith G, Strauss R 1985.
488 Morphometrics in evolutionary biology. Academy of Natural Sciences Press,
489 Philadelphia, PA, USA.
490
491 Cangelosi R, Goriely A 2007. Component retention in principal component analysis
492 with application to cDNA microarray data. Biology Direct 2, 1-21.
493
494 Clauss M, Hofmann RR, Fickel J, Streich WJ, Hummel J 2009. The intraruminal
495 papillation gradient in wild ruminants of different feeding types: Implications for rumen
496 physiology. Journal of Morphology 270, 929–942.
497
498 Clauss M, Hofmann RR, Streich WJ, Fickel J, Hummel J 2010a. Convergence in the
499 macroscopic anatomy of the reticulum in wild ruminant species of different feeding
500 types and a new resulting hypothesis on reticular function. Journal of Zoology 281,
501 26–38.
502
503 Clauss M, Hume ID, Hummel J 2010b. Evolutionary adaptations of ruminants and
504 their potential relevance for modern production systems. Animal 4, 972–992.

505

506 Deng Q, Zhou M, Wu Z 2010. An automatic non-rigid registration method for dense
507 surface models. Paper presented at the 2010 IEEE International Conference on
508 Intelligent Computing and Intelligent Systems, 29-31 October 2010, Xiamen, China.
509 pp 888-892.

510

511 Goopy P, Donaldson A, Hegarty R, Vercoe PE, Haynes F, Barnett M, Oddy VH 2013.
512 Low-methane yield sheep have smaller rumens and shorter rumen retention time.
513 British Journal of Nutrition 111, 578–585.

514

515 Hammond KJ, Pacheco D, Burke JL, Koolaard JP, Muetzel S, Waghorn GC 2014.
516 The effects of fresh forages and feed intake level on digesta kinetics and enteric
517 methane emissions from sheep. Animal Feed Science and Technology 193, 32-43.

518

519 Heimann T, Meinzer HP 2009. Statistical shape models for 3d medical image
520 segmentation: A review. Medical Image Analysis 13, 543-563.

521

522 Hofmann RR 1989. Evolutionary steps of ecophysiological adaptation and
523 diversification of ruminants: a comparative view of their digestive system. Oecologia.
524 78, 443–457.

525

526 Jackson DA 1993. Stopping rules in principal components analysis: a comparison of
527 heuristical and statistical approaches. Ecology Society of America 74, 2204-2214.

528

529 Janssen PH 2010. Influence of hydrogen on rumen methane formation and
530 fermentation balances through microbial growth kinetics and fermentation
531 thermodynamics. Animal Feed Science and Technology 160, 1-22.
532
533 Kendall D 1977. A survey of the statistical theory of shape. Statistical Science 4, 87–
534 120.
535
536 Pacheco D, Waghorn G, Janssen PH 2014. Decreasing methane emissions from
537 ruminants grazing forages: a fit with productive and financial realities? Animal
538 Production Science 54, 1141-1154.
539
540 Pinares-Patiño CS, Ulyatt MJ, Lassey KR, Barry TN, Holmes CW 2003. Rumen
541 function and digestion parameters associated with differences between sheep in
542 methane emissions when fed chaffed lucerne hay. Journal of Agricultural Science
543 (Cambridge) 140, 205–214.
544
545 Pinares-Patiño CS, McEwan JC, Dodds KG, Cárdenas EA, Hegarty RS, Koolaard,
546 JP, Clark H 2011a. Repeatability of methane emissions from sheep. Animal Feed
547 Science and Technology. 166, 210-218.
548
549 Pinares-Patiño CS, Ebrahimi SH, McEwan JC, Dodds KG, Clack H, Luo D 2011b. Is
550 rumen retention time implicated in sheep differences in methane emission?
551 Proceedings of the New Zealand Society of Animal Production 71, 219–222.
552

553 Pinares-Patino CS, Hickey SM, Young EA, Dodds, KG, MacLean S, Molano G,
554 Sandoval E, Kjestrup H, Harland R, Hunt C, Pickering NK, McEwan JC 2013.
555 Heritability estimates of methane emissions from sheep. Animal 7, 316–321.
556
557 Rosenberger AL 2011. Evolutionary morphology, platyrrhine evolution, and
558 systematics. The Anatomical Record 294, 1955–1974.
559
560 Schneider MTY, Zhang J, Crisco JJ, Weiss APC, Ladd AL, Nielsen P 2015. Men and
561 women have similarly shaped carpometacarpal joint bones. Journal of Biomechanics
562 48, 3420–3426.
563
564 Sellers AF, Stevens CE 1966. Motor functions of the ruminant forestomach.
565 Phsiological Reviews 46, 634–661.
566
567 Sutherland TM 1988. Particle separation in the forestomachs of sheep. In Aspects of
568 digestive physiology in ruminants (ed A Dobson), pp. 43-73. Cornell University Press,
569 Ithaca, NY, USA.
570
571 Treece GM, Prager RW, Gee AH 1999. Regularised marching tetrahedra: improved
572 iso-surface extraction. Computers and Graphics 23, 583-598.
573
574 Waghorn GC. Reid CSW 1977. Rumen motility in sheep and cattle as affected by
575 feeds and feeding. Proceedings of the New Zealand Society of Animal Production 37,
576 176-181.
577

578 Waghorn, GC and Reid, CSW 1984. Bloat in cattle 43. Resting level and vertical
579 displacement of the cranial pillar and other structures in the rumino reticulum of cattle of
580 known bloat susceptibility. New Zealand Journal of Agricultural Research 27, 481-490.
581
582 Webster M, Sheets HD, 2010. A practical Introduction to landmark-based geometric
583 morphometrics. Quantitative methods in paleobiology, 16,168-188.
584
585 Wiley DF, Amenta N, Alcantara DA, Ghosh D, Kil YJ, Delson E, Harcourt- Smith E,
586 Rohlf FJ, St John K, Hamann D 2005. Evolutionary morphing. Paper presented at
587 IEEE Visualization, 23-28 October 2005, Minneapolis, MN, USA, pp. 431- 438.
588
589 Wyburn RS 1980. The mixing and propulsion of the stomach contents of ruminants.
590 In Digestive physiology and metabolism in ruminants (ed Y Ruckebusch and P
591 Thivend), pp. 35-51. AVI Publishing Company, Westport, CT, USA.
592
593 Zelditch ML, Donald L, Swiderski H. Sheets D, Fink WL 2004. Geometric
594 morphometrics for biologists: a primer. Elsevier Academic Press, Massachusetts,
595 MA, USA.
596
597 Zhang J, Malcolm D, Hislop-Jambrich J, Thomas CDL, Nielsen P 2013. An
598 anatomical region-based statistical shape model of the human femur. Computer
599 Methods in Biomechanics and Biomedical Engineering: Imaging & Visualization 2,
600 176–185.
601

602 Zhang J, Hislop-Jambrich T, Besier J 2016. Predictive statistical models of baseline
603 variations in 3D femoral cortex morphology. Medical Engineering and Physics 38,
604 450-457.
605